

Analysis of Connecting Rod for Static Stress and Deformation for Different Materials

Sourabh Mishra¹, Ruchika Saini², U. K. Joshi³

¹Research Scholar, ²Assistant Professor, ³Associate Professor,
Department of Mechanical Engineering, JEC, Jabalpur, Madhya Pradesh, India.

Abstract:- In the ever-evolving field of automotive engineering, the connecting rod assumes a pivotal role in the seamless transformation of reciprocating piston motion into the rotary motion that propels an engine's crankshaft. Traditionally crafted from carbon steel, recent strides in materials science have unveiled the potential of aluminium alloys as a compelling alternative. These alloys, lauded for their lightweight attributes and remarkable impact resistance, particularly excel in the demanding realm of high-speed motorcycle engines. This study undertakes an exhaustive examination of four distinct aluminium alloy materials—AA7068, AA6061, and AA6061-9%Si-15%Fly ash, A356-5%Si-10%Fly ash—employing Finite Element Analysis (FEA) conducted via ANSYS software. Our investigation meticulously assesses crucial parameters including von Mises stress, Equivalent Elastic Strain and total Deformation.

Keywords:- ANSYS Workbench 2022 R1, Connecting Rod, SolidWorks 2021, Deformation Analysis, Static Structural Analysis, Stiffness, Aluminium Alloy.

I. INTRODUCTION

The connecting rod serves as a fundamental and indispensable component within internal combustion engines (IC), acting as the link pin in the conversion of reciprocating motion into rotational power. This critical link bridges the piston and the crankshaft, enduring substantial mechanical stresses throughout the engine's operation. The performance and durability of any IC engine are intricately tied to the structural integrity and material composition of its connecting rod[1]–[4].

Traditionally crafted from materials like steel, recent strides in materials science have ushered in a plethora of alternatives, including a diverse array of alloys and composite materials. These emerging materials offer the tantalizing prospect of enhancing the strength-to-weight ratios, bolstering durability, and reducing the overall weight of IC engines. These attributes are paramount in the pursuit of optimized engine performance and enhanced fuel efficiency[5], [6],[7]

This study embarks on a comprehensive analysis of connecting rods, with a specific focus on evaluating their static stress and deformation behaviours under varying loading conditions, leveraging an assortment of materials. The selected materials encompass a wide spectrum of alloys,

composites, and innovative substances, each possessing distinct properties that can profoundly influence how the connecting rod responds to mechanical stress[8], [9].

By amalgamating analytical calculations with advanced simulation techniques, we aim to dissect the influence of different materials on stress distribution and deformation patterns within the connecting rod. The culmination of this analysis seeks to provide invaluable insights into the suitability of various materials for connecting rod applications. Ultimately, our findings will serve as a guiding beacon in the selection of materials that deliver optimal performance, safety, and efficiency within the realm of IC engines. This research endeavours to contribute to the continual advancement of IC engine design, fostering the development of sustainable and high-performance automotive technologies[10]–[13].

Adoption of alternative materials across multiple sectors is crucial for sustainable industrial growth. Hybrid materials, which combine two or more reinforcements to improve mechanical qualities including stiffness, strength, and high strength-to-weight ratios, are one such novel technique. Incorporating inexpensive elements with various properties into a matrix phase is the conventional method for producing hybrid materials. Due to their light weight and high strength characteristics, hybrid metal matrix composites, a cutting-edge class of materials, find applications in the aerospace and automotive industries. These hybrid metal matrix composites are made using a variety of production processes, such as stir casting and stir cum squeeze casting[14]–[17].

In the context of internal combustion engines, the connecting rod plays a pivotal role, serving as an intermediary link between the piston and the crankshaft. During engine operation, this component must withstand compressive and tensile loads. In the past, materials like carbon steel, alloy steels, magnesium alloys, aluminium alloys, and titanium alloys have been used to make connecting rods. The choice of material is influenced by things like the load and performance demands of the engine. For instance, alloy steel is favoured for high-performance engines due to its cyclic strength without dimensional changes, whereas carbon steel is suited for mild loads. In contrast, connecting rods made of magnesium and aluminium alloys offer a significant weight reduction of 20% to 25% over steel. Titanium alloy connecting rods are preferred for use in high-performance turbocharged engines

due to their superior strength and fatigue characteristics and lower density than steel[18]–[20].

Finite element analysis (FEA) has been used in earlier studies in this area to evaluate the stress and deformation properties of connecting rods in internal combustion engines. Connecting rods composed of various materials, including as steel, aluminium alloys, and even composite materials, have been the subject of several investigations. These studies sought to improve connecting rod design, lessen weight, and guarantee safety under various loading scenarios. Understanding the behaviour of connecting rods under various stresses and loads has shown to be a valuable use of FEA[21]–[23].

These loads are considerably more relevant in modern engines because they have higher torque values at slower rotational speeds. Therefore, the focus of this study is on applying the finite element technique (FEM) to undertake static stress analysis of connecting rods. The inquiry will focus on four different materials: A356, A356-5%SiC-10% Fly ash stir cum squeeze casting, A356-5%SiC-10% Fly ash stir casting, and Al2024-T3. In order to learn more about the structural integrity and performance of these connecting rods under various loading circumstances, the analysis is carried out using the ANSYS finite element code. In order to improve the robustness and efficiency of internal combustion engines, it is intended to provide useful insights into design and material selection[24]–[26].

Numerous investigations are still looking for robust and lightweight materials for the connecting rod parts that are under the most strain, according to reviews of the literature. These studies have more of an emphasis on examining the design of connecting rods for two-wheelers constructed of diverse materials. Since the current study involves the modelling of connecting rod using Solid Works and ANSYS Workbench was used to investigate various materials, the analytical and numerical findings for the various materials used are evaluated. As a result, it is advised to use these composites to make connecting rods for motorcycles[27]–[30].

II. ANALYTICAL PROCEDURE

➤ *Materials.*

Metal Alloys, contain aluminium (Al). alloying elements comprising copper, magnesium, silicon, tin, zinc, and manganese. In engineering structures where lightweight and corrosion resistance are important, aluminium alloys are widely utilised. Two aluminium alloys and composites—AA6061, AA7068, AA6061-9%sic-15%Fly ash, and A356-5

percent Sic-10 percent fly ash stir cum squeeze casting—are considered in this study[1].

- *AA6061 Aluminium Alloy.*
Type AA6061 aluminium has a nominal composition of 97.98% Al, 0.61% Si, 1.15% Mg, 0.19% Cr, and 0.27% Cu. Aluminium alloy 6061 has a density of 2.7 g/cm³ (0.0975 lb/in³). Heat treatable, readily made, weldable, and good at resisting corrosion, 6061 aluminium alloy.

- *AA7068 Aluminium Alloy.*
AA7068 aluminium alloy has a nominal composition of 8.98% Zn, 2.99% Mg, 2.5% Cu, 0.16% Fe, 0.16% Zr, 0.11% Si, 0.2% Mn, 0.15% Ti, 0.05% Cr, 0.15% other, 85.48% Al, A common aluminium alloy called aluminium 7068 is renowned for its toughness, longevity, and resistance to corrosion. For applications requiring very precise parts with exceptional tensile strength, it is employed in the automotive and aerospace sectors. As a result of this alloy's high formability qualities, it is also regarded as one of the most weldable aluminium alloys.

- *AA6061-9%SiC-15%Fly Ash Aluminium Alloy.*
This is an aluminium alloy primarily composed of aluminium (Al), magnesium (Mg), and silicon (Si). AA6061 is known for its good strength-to-weight ratio, corrosion resistance, and weldability. It is commonly used in various engineering applications, including aerospace, automotive, and structural components. 9% SiC (Silicon Carbide) and 15% Fly ash - Silicon Carbide (SiC) and Fly ash are added to the aluminium alloy matrix as reinforcements to improve certain mechanical properties, SiC is a ceramic material known for its high hardness, strength, and excellent wear resistance. Fly ash is a fine powder residue generated from the combustion of coal in power plants. It contains various minerals and silicates. When incorporated into the aluminium alloy, Fly ash can act as a filler or reinforcement, potentially improving properties like thermal stability and reducing cost.

- *A356-5%SiC-10%Fly Ash Aluminium Alloy.*
The A356-5%SiC-10%Fly ash aluminium alloy composite combines A356 aluminium alloy's excellent castability with 5% silicon carbide (SiC) for enhanced hardness, strength, and wear resistance, ideal for applications needing improved mechanical properties. Additionally, the incorporation of 10% Fly ash, a coal combustion byproduct, serves as a potential cost-effective filler and can enhance properties like thermal stability. The specific performance characteristics of this composite depend on manufacturing processes and the precise proportions of its components.

Table 1 Connecting Rod Material Properties.

Parameter	A356-5%SiC-10%Fly ash	AA7068	AA6061	AA6061-9%SiC-15%Fly ash
Density(kg/m ³)	4272	2850	2700	2611.6
Young Modulus E (Mpa)	114720	73100	68900	70000
Poisson's Ratio	0.35	0.23	0.33	0.33
Tensile Yield Strength (Mpa)	308	590	276	363
Ultimate Tensile Strength (Mpa)	408	641	310	422

➤ *Engine Technical Specifications.*

The connecting rod dimensions used in this project were drawn from the TVS Motorcycle-Apache RTR 150cc standard engine, which has the following engine specifications discussed in table 2.

Table 2 Engine Technical Specification (150 Cc TVS Apache RTR Engine)[11].

Engine Type.	Fan Cooled 4-Stroke.
Displacement(cc).	147.5cc
Bore * Stroke (Mm).	57*57.8 mm
Maximum Power.	9.95 kW @ 8500 rpm
Maximum Torque.	12.4 kW @ 6000 rpm
Compression Ratio.	9.5:1
Density Of Petrol.	737.22 kg/m ³
Power To Weight Ratio	101.7 bhp/ton

➤ *Boundary Calculation.*

• *Constants:*

- ✓ Molar mass of Petrol (C₈H₁₈) = 0.11423 kg/mol
- ✓ Universal Gas Constant (R) = 8.314 J/(mol·K)
- ✓ Auto ignition temperature (T) = 553.15 K
- ✓ Volume (V) = Displacement Volume, V_s = 0.0001475 m³
- ✓ Acceleration due to gravity (g) = 9.818 m/s²
- ✓ Gear ratio (n) = 4
- ✓ Time (t) = 1 second.

• *Calculations:*

- ✓ mass = Power / Power-to-weight ratio.
- ✓ mass = 9.95 kW / (101.6 bhp/ton) × 1000 kg/ton ≈ 0.0978 kg.
- ✓ Specific Gas Constant (R_{specific}):
- ✓ R_{specific} = R / M = 8.314 / 0.11423 ≈ 72.787

• *Gas Pressure (P):*

- ✓ $P = (\text{mass} \times R_{\text{specific}} \times T) / V$
- ✓ $P = (0.0978 \text{ kg} \times 72.787 \times 553.15) / 0.0001475 \text{ m}^3 \approx 29.87 \text{ MPa}$

• *Angular Velocity (ω):*

✓ $\omega = (2\pi \times \text{RPM}) / 60 = (2\pi \times 8500) / 60 \approx 892.699 \text{ rad/s.}$

• *Angle of Rotation (ϕ):*

✓ $\phi = (2\pi \times \text{RPM}) / 60 \times \text{time} = (2\pi \times 8500) / 60 \times 1 \approx 895.98 \text{ rad}$

• *Force of Inertia (FI):*

- ✓ $FI = m \times \omega^2 \times r \times (\cos(\phi) + \cos(2\phi) / n).$
- ✓ $FI = 0.0978 \text{ kg} \times (892.699 \text{ rad/s})^2 \times 0.0289 \text{ m} \times (\cos(895.98 \text{ rad}) + \cos(2 \times 895.98 \text{ rad}) / 4)$
- ✓ $FI \approx 3439.49 \text{ N.}$

• *Total Force acting (F):*

- ✓ Given FP = 39631.19133 N and FI = 3439.49 N.
- ✓ $F = FP - FI \approx 36191.70133 \text{ N.}$

➤ *Deformation and Stiffness Calculation.*

- Length = 140 mm.
- The connecting rod's thickness (t) = 3.075 mm.
- Area of connecting rod = 11 t².
- Stress = P/A = 36192 / (11*3.075²) = 350 Mpa.

Table 3 Connecting Rod's Deformation and Stiffness Calculation.

Material	Deformation (mm) $\Delta L = (\sigma_t * L) / E$	Weight (Kg.)	Stiffness (Weight/Deformation) Kg/mm
AA7068	0.67031	0.6431	0.95543
AA6061	0.7111	0.221	0.3107
AA6061-9%SiC-15%Fly ash	0.7000	0.2139	0.30557
A356-5%SiC-10%Fly ash	0.4271	0.35	0.49166

➤ *Modelling of Connecting Rod.*

Based on the dimensions modal of the connecting rod developed with the Solid works 2021 programme, the solid modal of a connecting rod from a two-wheeler with a 150 cc four-stroke single cylinder engine is selected for analysis. It is imported into Ansys 2022R1. Figure 1,2 and 3 shows the dimensions, model, and meshing of the Connecting Rod.

Meshing is the process of disassembling intricate geometry into more manageable components. It has an

impact on the simulation's convergence, accuracy, and speed. In this case, the tetrahedron mesh method with a 1 mm element size is applied. 1028097 nodes, with a total of 717208 elements, are applied.

Applying the boundary condition comes after meshing the model. By securing the crank end and applying a compressive force of 36192 N to the piston end in accordance with thermodynamic, we have only taken Two case piston finish According to thermodynamics, the power

stroke is the third stage of an IC engine. Burning the air-fuel combination is the crucial phase of a thermodynamic cycle. In this, the connecting rod's movement under a power stroke condition is examined. Different materials apply the same boundary condition, and a solution is found.

- Thickness of flange, $t = 3.075$ mm.
- Width of section, $B = 4 t = 12.33$ mm.
- Depth or height of section, $H = 5 t = 15.375$ mm.
- Depth near big end, $H1 = 18.066$ mm.
- Depth near small end, $H2 = 12.684$ mm.[11]

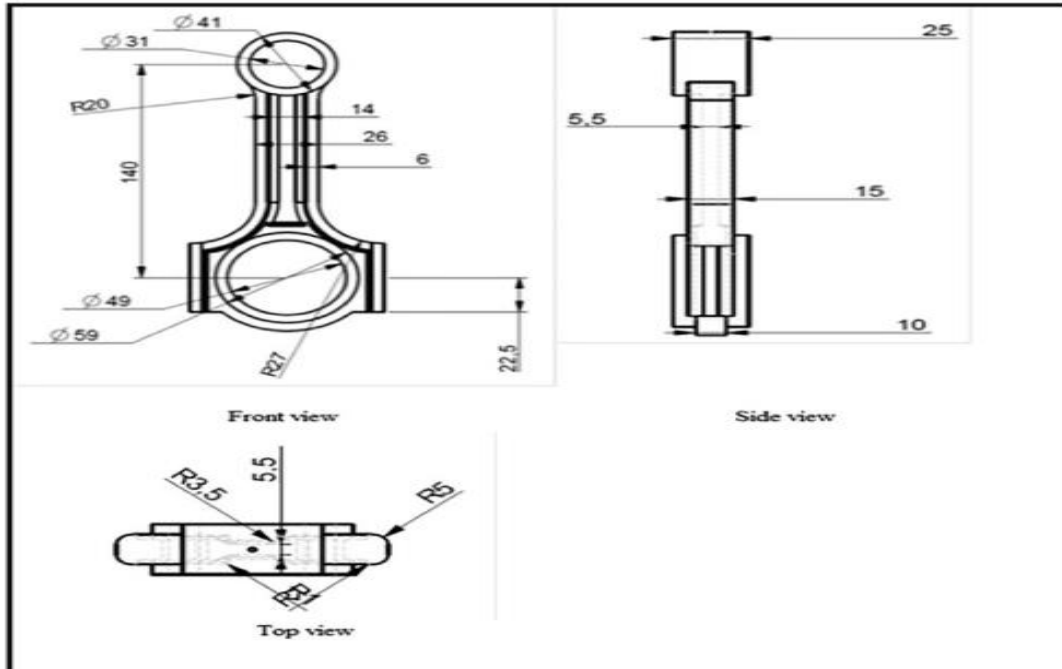


Fig 1 Dimensions of Connecting Rod.

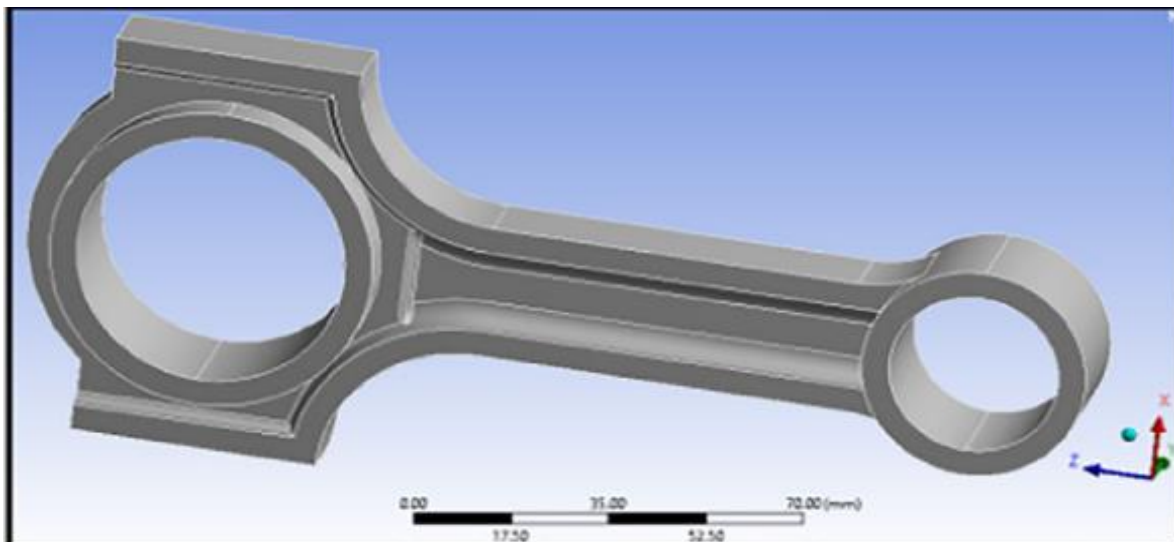


Fig 2 Model of Connecting Rod.

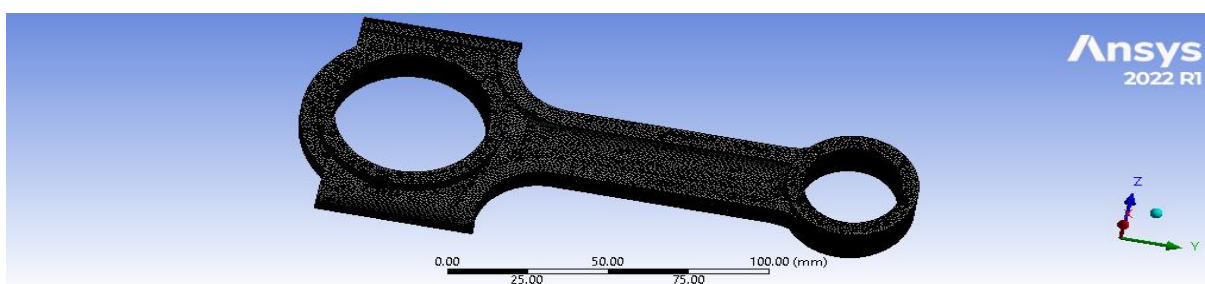


Fig 3 Meshing Model of Connecting Rod.

III. RESULTS AND DISCUSSION

➤ *Analysing the Various Outcomes.*

Table 4 Indicate the ansys static structural analysis result for deformation, equivalent stress, and equivalent elastic strain results for all the respective materials, the AA7068 has the least deformation and the highest stiffness, followed by the aluminium alloys A356-5%SiC-10%Fly ash, AA6061, and AA6061-9%SiC-15%Fly ash.

The Figure 4 shows the fixed support at crank end, and figure 5 shows that the 36191N compressive load applied on piston end.

The Fig. 6 (a)-9 (a) shows the total deformation of materials AA6061, A356-5 %SiC-10 %fly ash, AA7068 and AA6061-9%SiC-15%Fly ash.

The Figs. 10 (a)-13 (a) shows the Equivalent elastic strain of materials AA6061, A356-5 %SiC-10. %fly ash, AA7068 and AA6061-9%SiC-15%Fly ash.

The Figs. 14 (a)-17 (a) shows the Equivalent stress of materials AA6061, A356-5 %SiC-10 %fly ash, AA7068 and AA6061-9%SiC-15%Fly ash.

Fig 18. Fig 19. And figures 20. Shows that variation of Deformation, Equivalent (von-mises) Stress, and Equivalent Elastic Strain from different Materials.

figure 21 and 22. Shows the theoretical and ansys result comparison values.

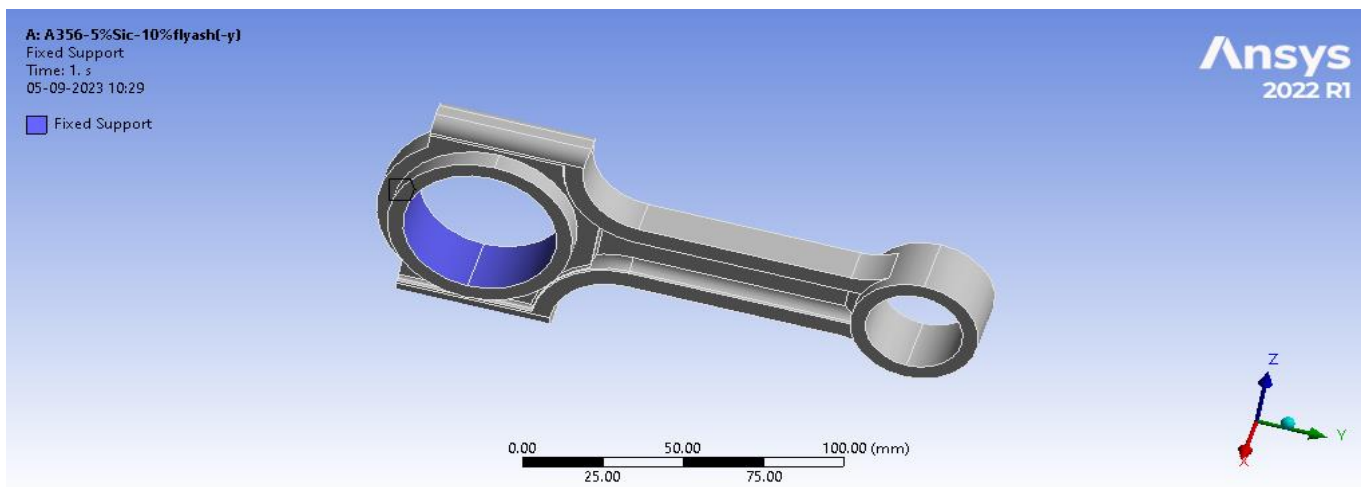


Fig 4 Crank End Fixed.

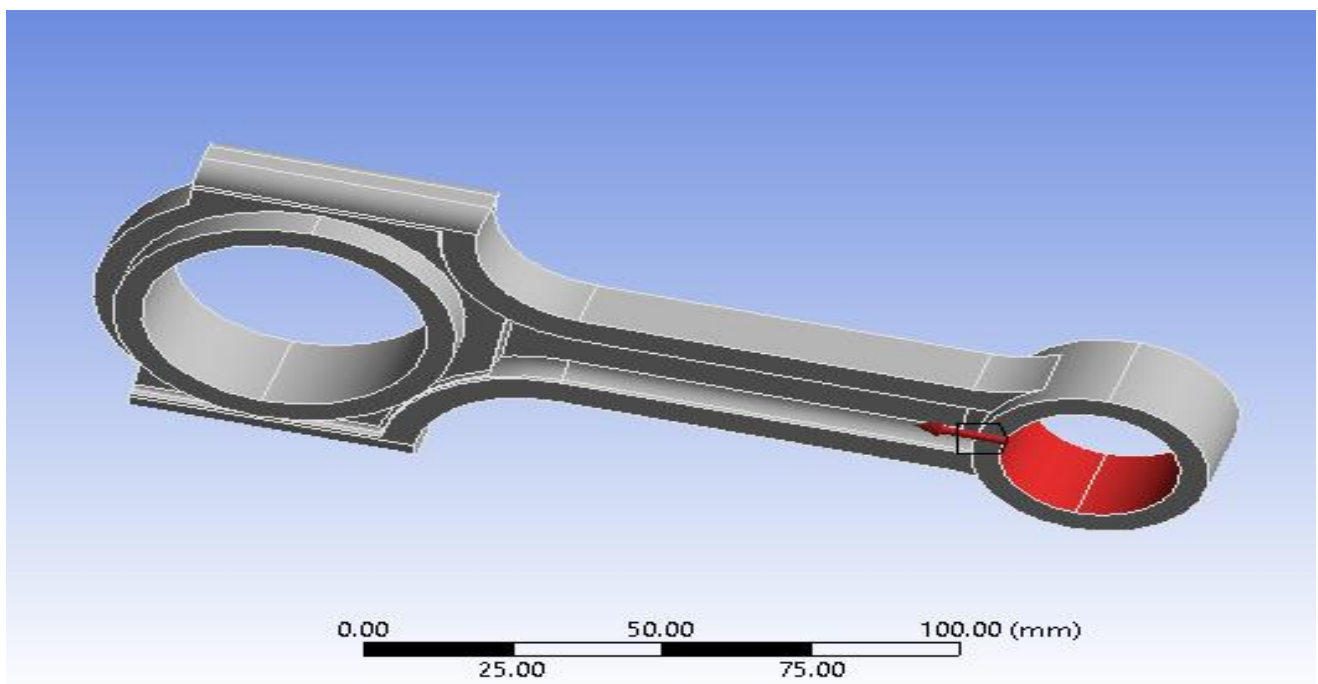


Fig 5 Compressive Load On Piston End.

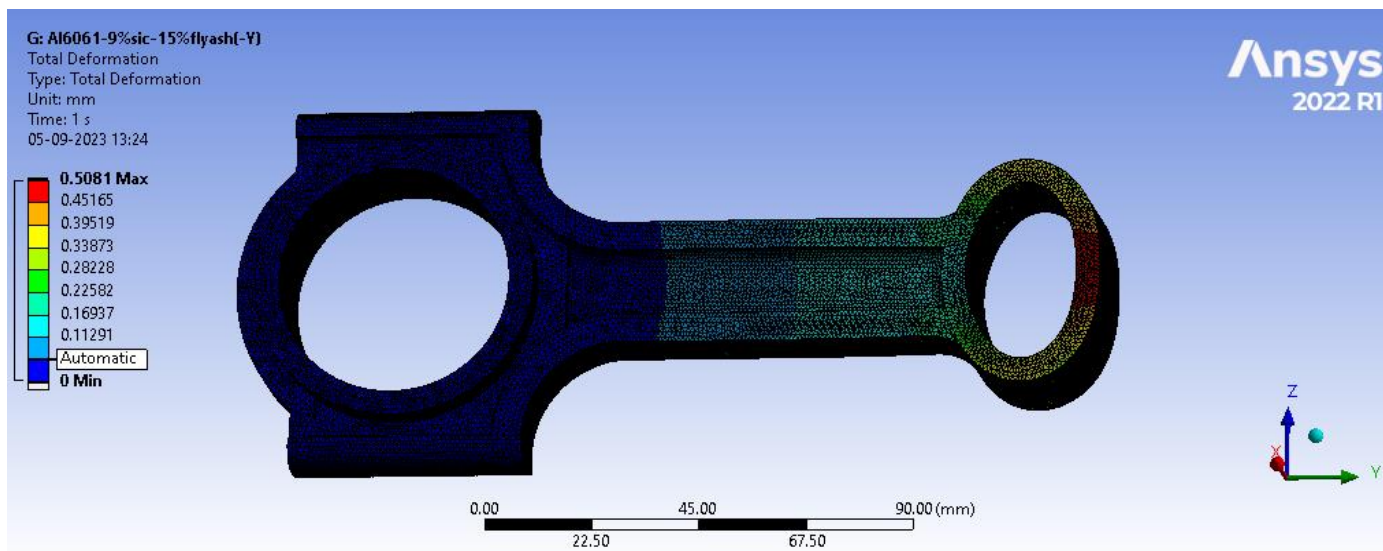


Fig 6 (a). Total Deformation Of AA6061-9%SiC-15%Fly Ash.

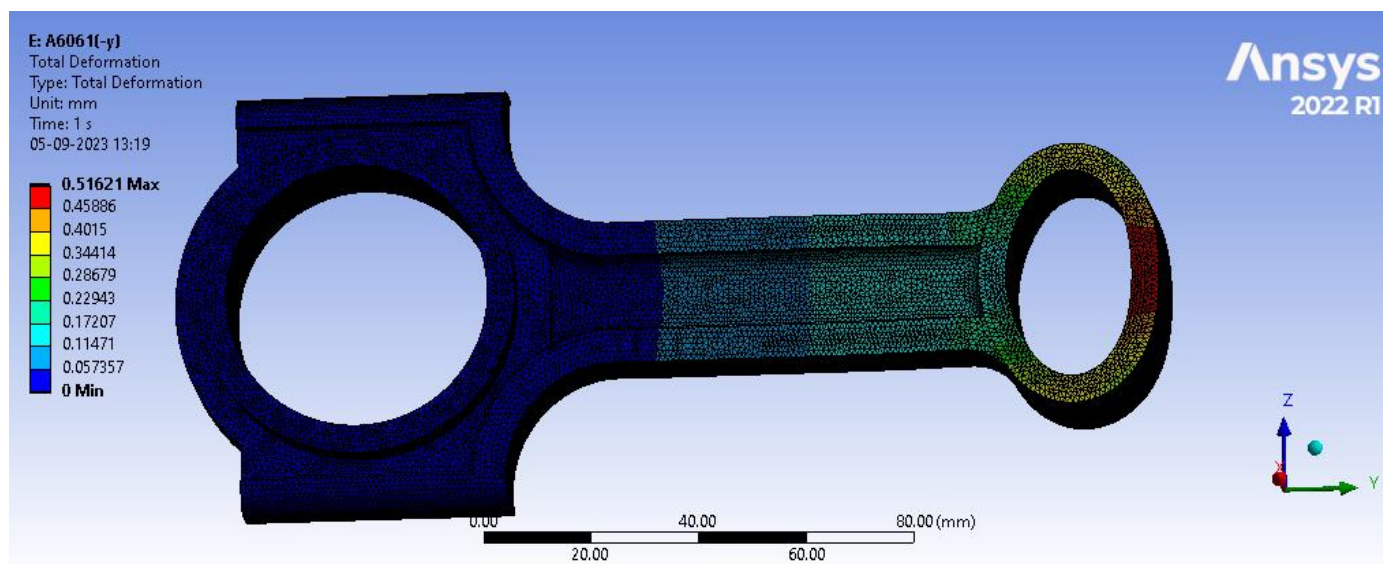


Fig 7 (a). Total Deformation Of AA6061.

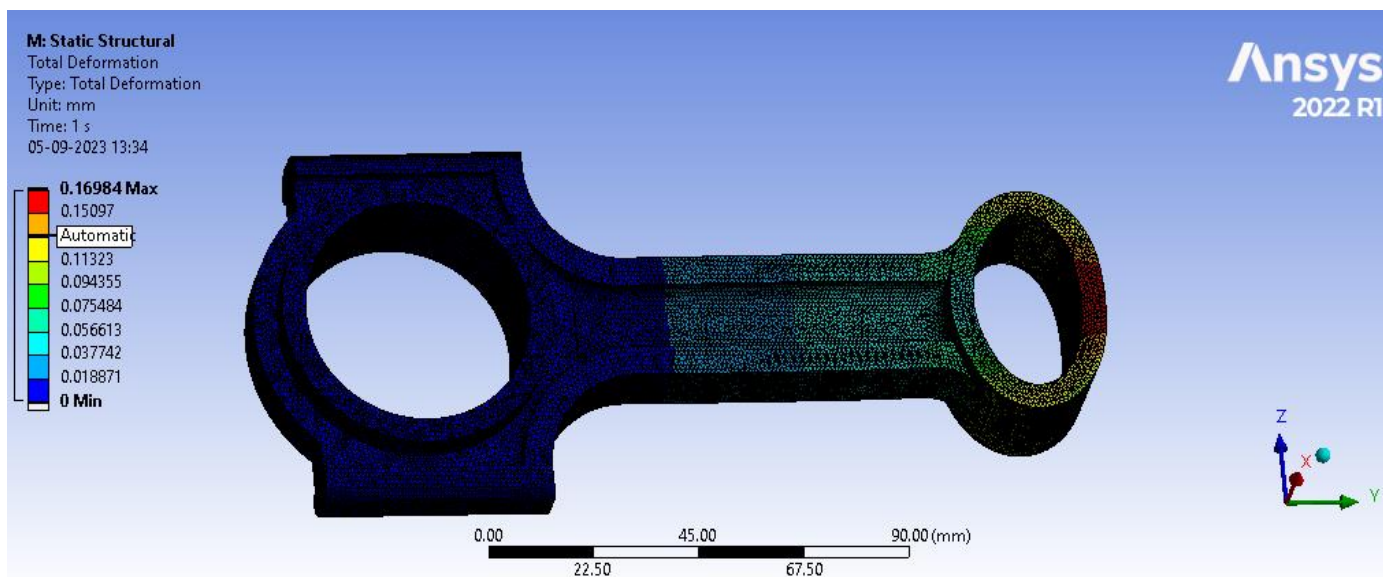


Fig 8 (a). Total Deformation of AA7068.

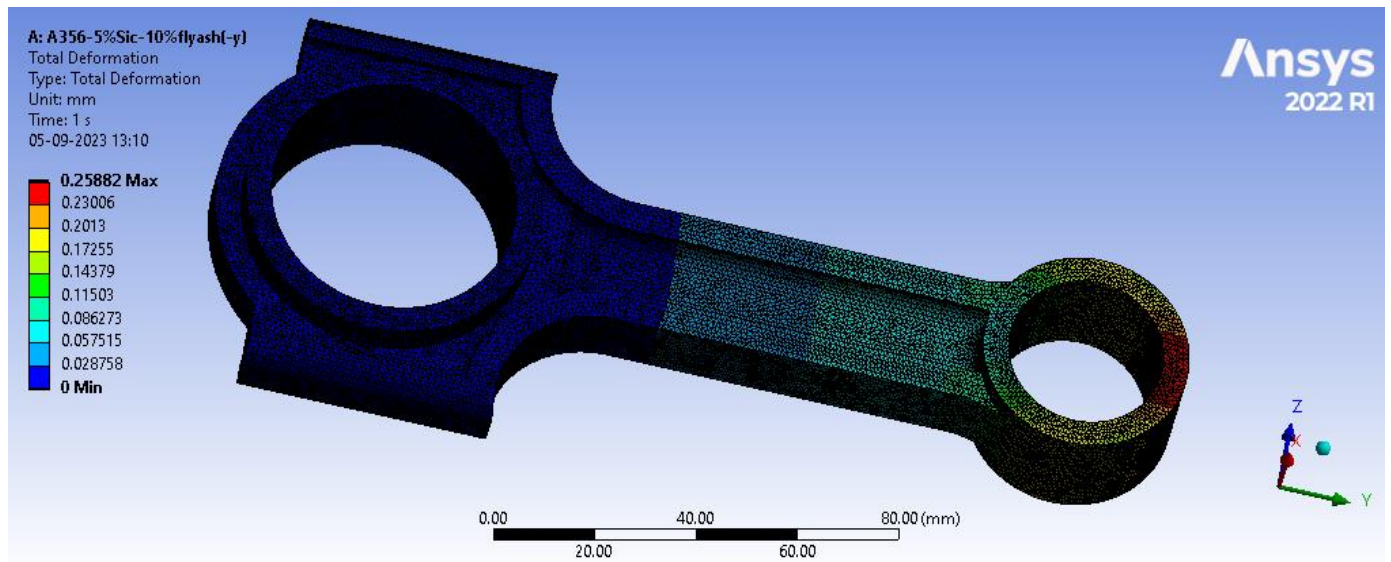


Fig 9 (a). Total Deformation of A356-5%SiC-10%Fly Ash.

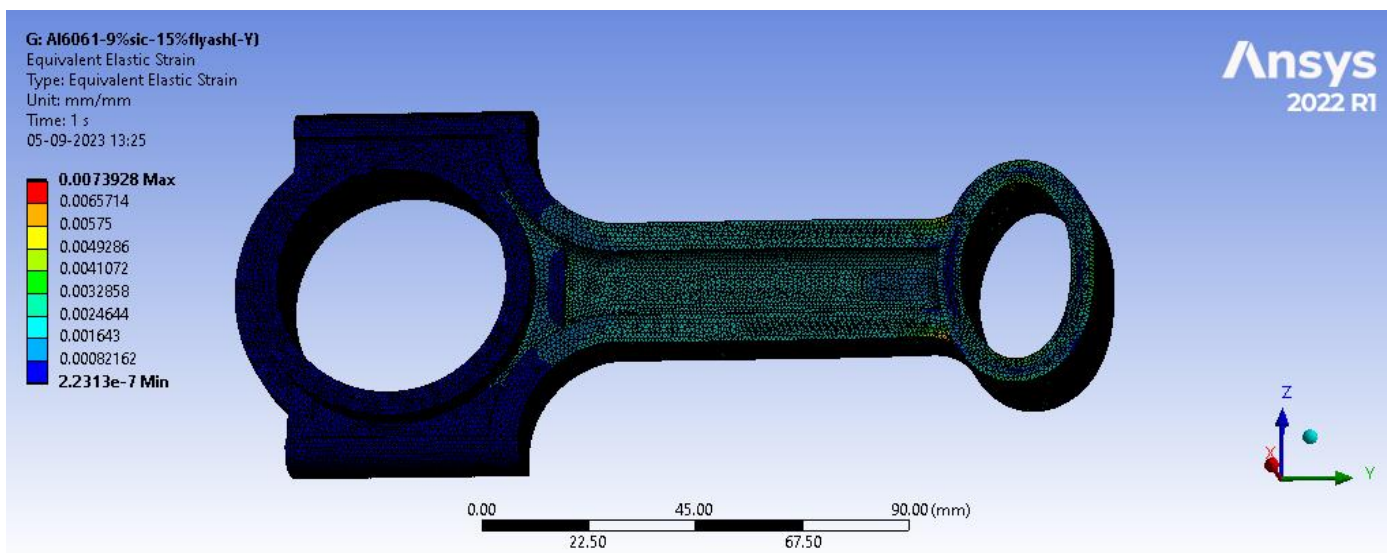


Fig 10 (a). Equivalent Elastic Strain of AA6061-9%SiC-15%Fly ash.

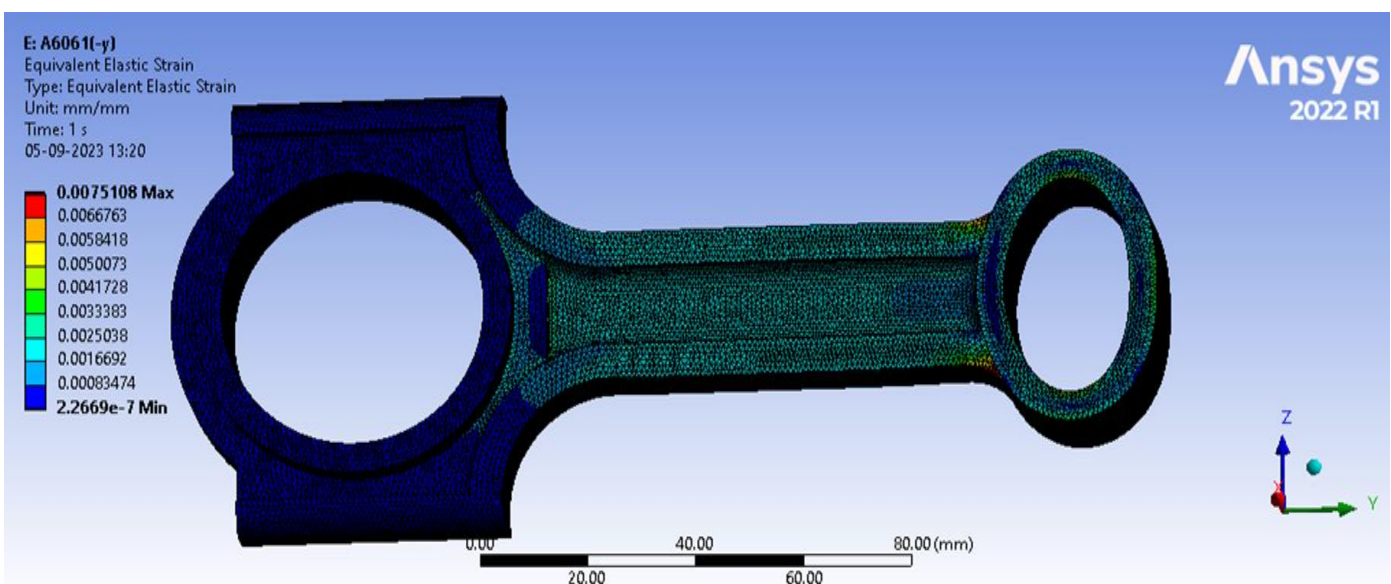


Fig 11 (a). Equivalent Elastic Strain of AA6061.

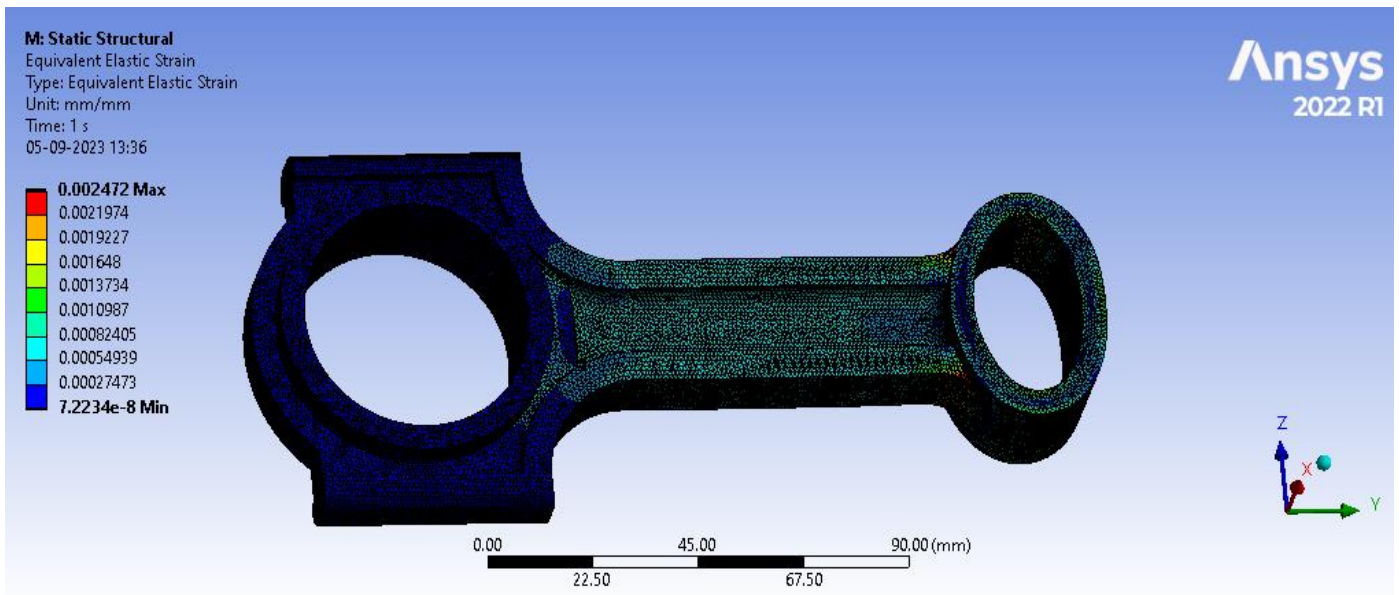


Fig 12 (a). Equivalent Elastic Strain of AA7068.

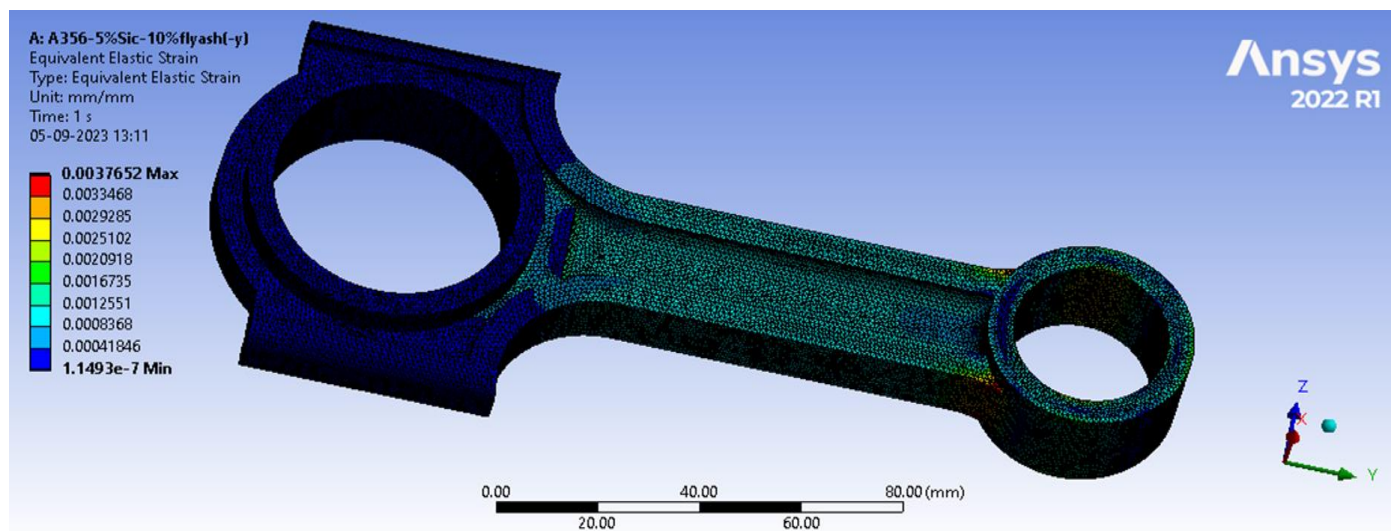


Fig 13 (a). Equivalent Elastic Strain of A356-5%SiC-10%Fly Ash.

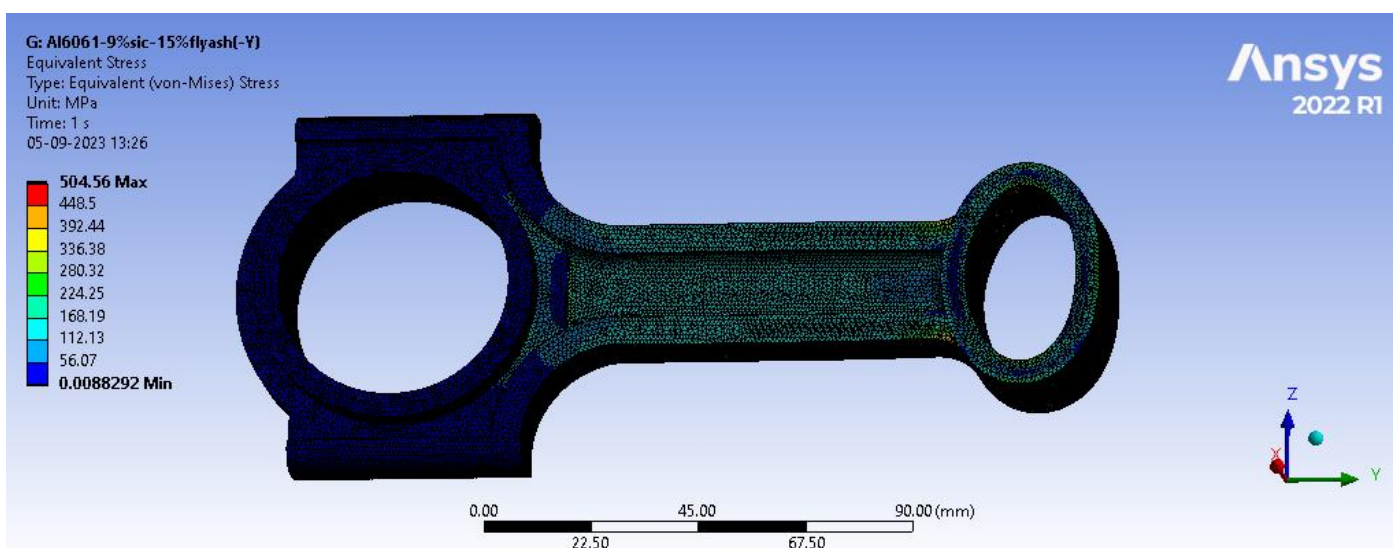


Fig 14 (a). Equivalent Stress of AA6061-9%SiC-15%Fly Ash.

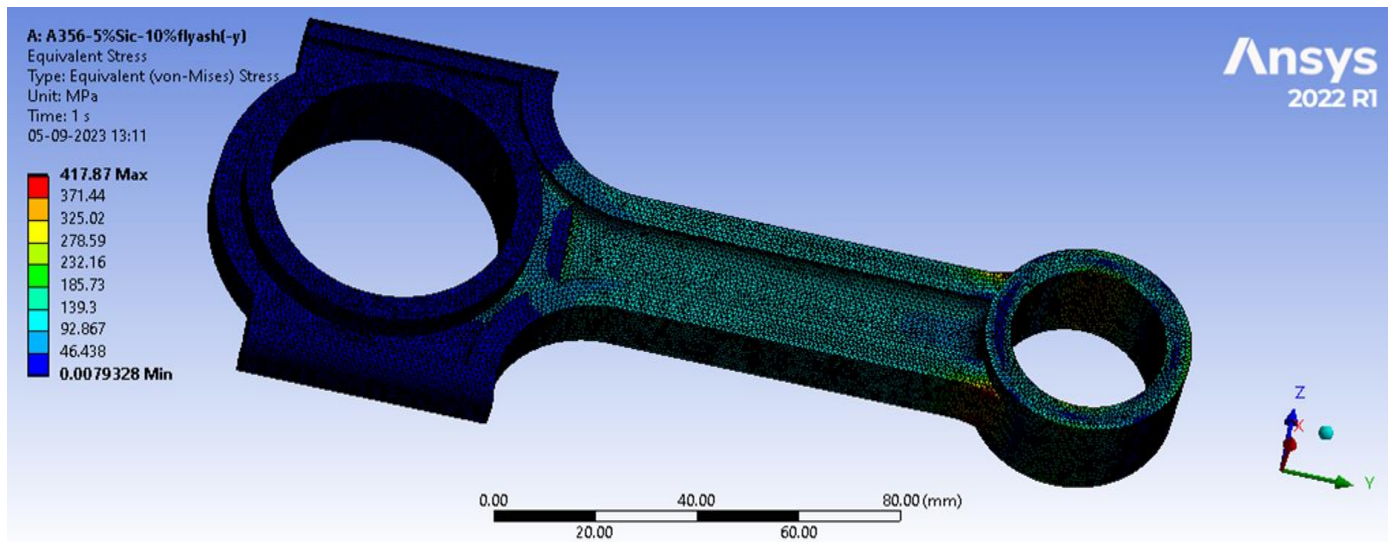


Fig 15 (a). Equivalent Stress of A356-5%SiC-10%Fly ash.

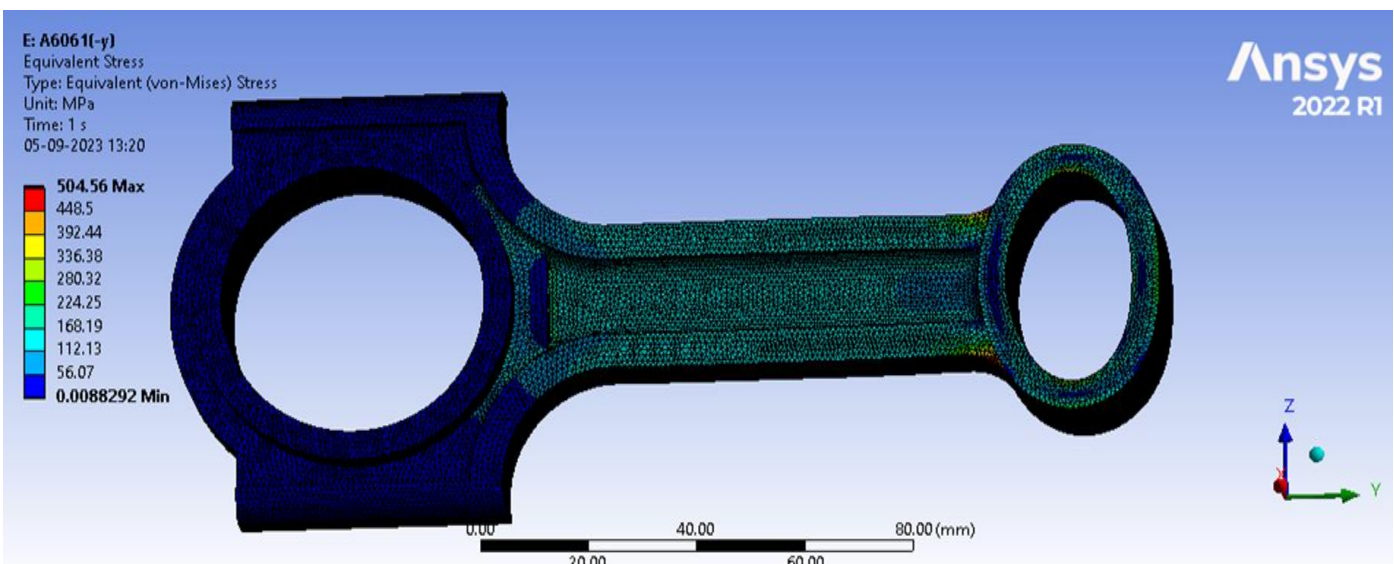


Fig 16 (a). Equivalent Stress of AA6061.

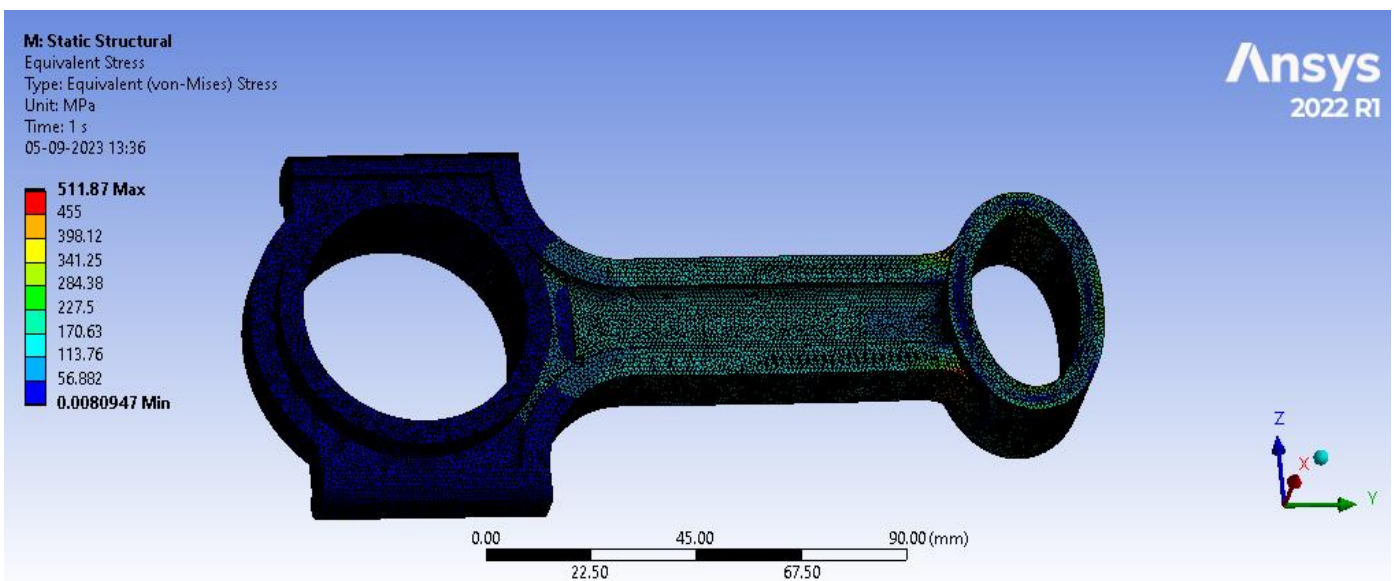


Fig 17 (a). Equivalent Stress of AA7068.

Table 4 Analysis Result of Connecting Rod.

Material	Total Deformation(mm)	Equivalent Elastic Strain(mm/mm)	Equivalent Stress (Mpa)
A356-5%SiC-10%Fly ash	0.25882	0.0037652	417.87
AA7068	0.16984	0.002472	511.87
AA6061	0.51621	0.0075108	504.56
AA6061-9%SiC-15%Fly ash	0.50811	0.0073928	504.56

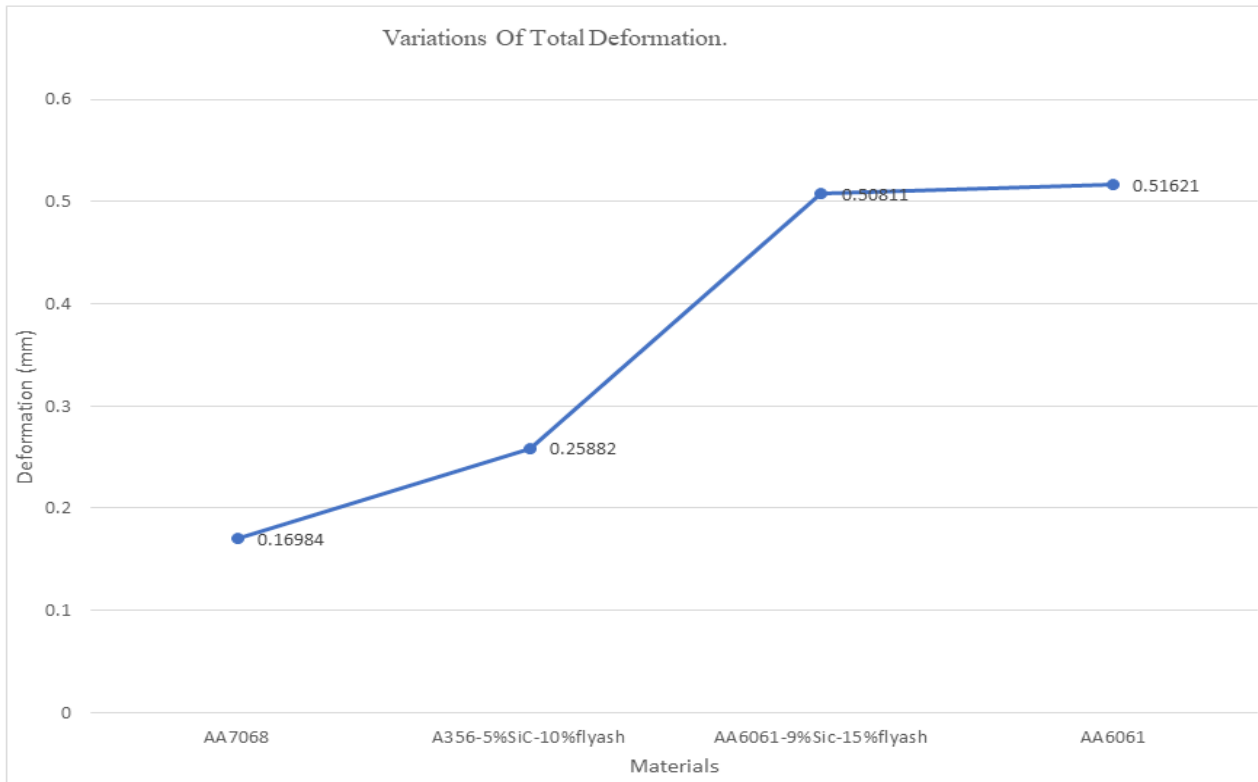


Fig 18 Variations of Total Deformation.

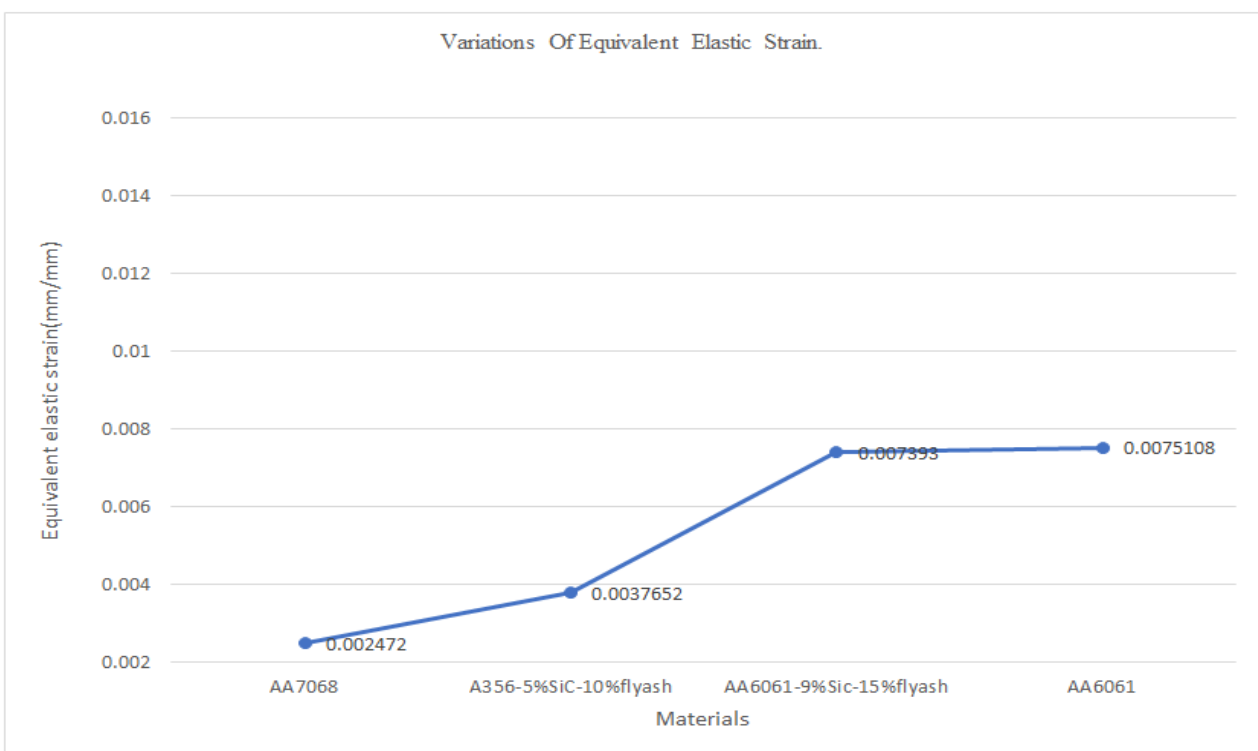


Fig 19 Variations of Equivalent Elastic Strain.

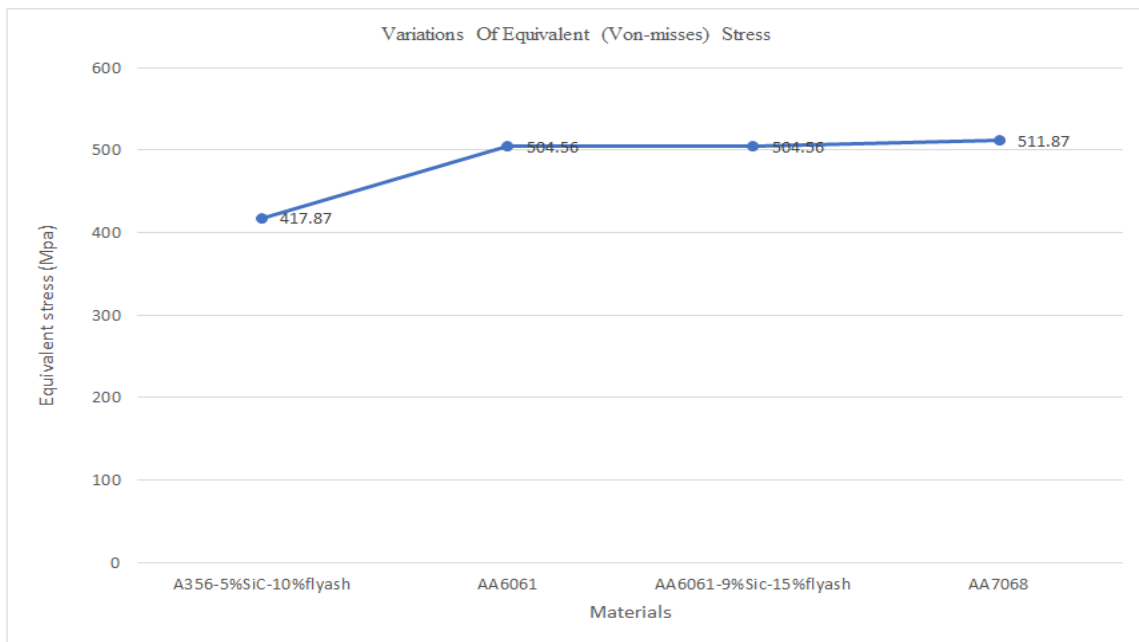


Fig 20 Variations of Equivalent (Von-Misses) Stress.

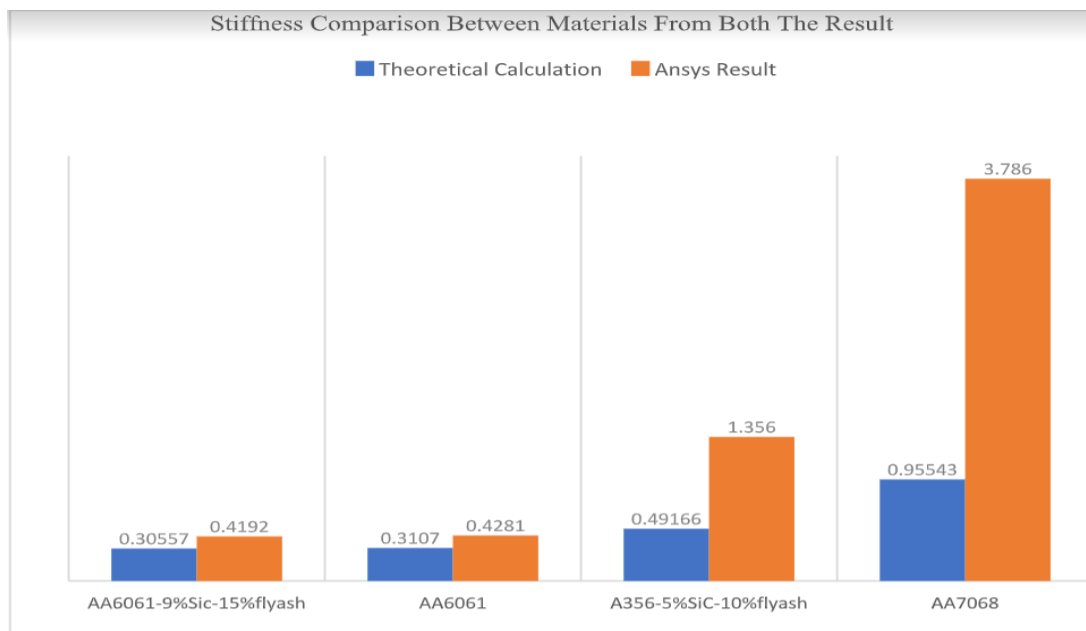


Fig 21 Stiffness Comparison between Materials from both the Result.

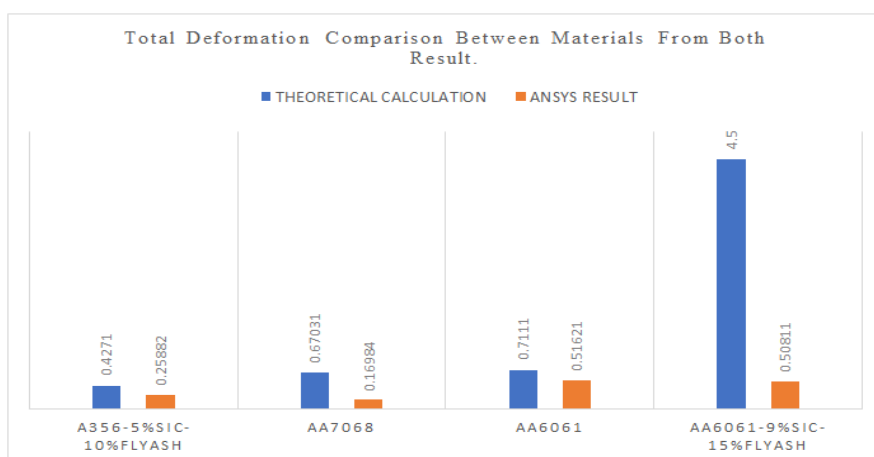


Fig 22 Total Deformation Comparison between Materials from both Result.

Table 5. Stiffness Calculation Results of the Connecting Rod.

Material	Deformation	Stiffness(N/mm)
A356-5%SiC-10%Fly ash	0.25882	1.356
AA7068	0.16984	3.7865
AA6061	0.51621	0.4281
AA6061-9%SiC-15%Fly ash	0.50811	0.4192

Table 6 Comparison of Results from Past Researchers.

Paper	Best Material	Engine chosen by Author	Total Deformation in mm	Elastic Strain mm/mm	Elastic Stress (Mpa)
In Ref. Paper[1]	A356-5%SiC-10%Fly ash	125 cc	0.3329	0.008849	1012.4
Our paper	AA7068	150cc	0.16984	0.002472	511.87

IV. DISCUSSION

Significant insights are revealed through the research of the connecting rod materials based on different mechanical properties. The connecting rod clearly faces compressive loads. The Majority of the time during a single thermodynamic cycle. AA7068 shows superior material qualities to AA6061, A356-5%SiC-10%Fly ash, and AA6061-9%SiC-15%Fly ash among the materials taken into consideration. This is underscored by its greater ultimate and compressive stress in both tensile and compression tests, as well as higher density, all of which point to a greater capability for carrying loads.

Numerical stress research also lends weight to these conclusions. With less overall deformation, equivalent elastic strain, and comparable von-Mises stress values, AA7068 regularly outperforms alternative materials. Compared to the other Materials, this material's overall deformation is reduced by about 60.73% in a comparison of reference paper. AA7068 and A356-5%SiC-10%Fly ash stir cum squeeze casting have analogous stress distributions that are quite similar, indicating similar structural behaviour.

As a result of these findings, it appears that AA7068 exhibits better mechanical performance, making it an attractive option for applications where load-bearing capacity and structural integrity are crucial. The study's conclusions offer useful guidance for choosing connecting rod materials in a variety of engineering applications.

V. CONCLUSION

Using the programmes Solid works 2021 and ANSYS Workbench 2022 R1, the connecting rod was successfully modelled and evaluated, and the results were presented as follows.

- The best connecting rod was AA7068 after the deformation and stiffness alternatives from theoretical and Ansys data were compared.
- Due to its low deformation, AA7068 provides a longer lifespan for connecting rods.
- Therefore, it may be concluded that connecting rods can be made from the AA7068 material.
- The results demonstrated that deformation can be decreased by modifying the materials.

- High von Mises stress gives the AA7068 aluminium alloy connecting rod have high impact strength.
- The best connecting rod out of four materials is AA7068 because of its good deformation characteristics (0.16984 mm) and high stiffness (3.7865 kg/mm).
- deformation is reduced by about 60.73% in a comparison of reference paper.

REFERENCES

- [1]. R. Kumar Verma and A. Kumar Jain, "Modelling and analysis of two-wheeler connecting rod with different materials using FEA," *Mater Today Proc*, vol. 62, no. P10, pp. 5867–5876, Jan. 2022, doi: 10.1016/j.matpr.2022.04.621.
- [2]. R. Kumar Verma and A. K. Jain, "Issue 12 www.jetir.org (ISSN-2349-5162)," 2021. [Online]. Available: www.jetir.org
- [3]. S. Ranganathan, S. Kuppuraj, K. Soundarajan, and A. Perumal, "Design and Analysis of Hybrid Metal Matrix Composite Connecting Rod via Stir/Squeeze Casting Route," in *SAE Technical Papers*, SAE International, Oct. 2019. doi: 10.4271/2019-28-0113.
- [4]. S. Seralathan *et al.*, "Stress analysis of the connecting rod of compression ignition engine," in *Materials Today: Proceedings*, Elsevier Ltd, 2020, pp. 3722–3728. doi: 10.1016/j.matpr.2020.06.137.
- [5]. S. Sharma and V. Gambhir, "Design and Comparative Performance Analysis of Two Wheeler Connecting Rod Using Two Different Materials Namely Carbon 70 Steel and Aluminum 7068 by Finite Element Analysis 4 PUBLICATIONS 4 CITATIONS SEE PROFILE Design and Comparative Performance Analysis of Two Wheeler Connecting Rod Using Two Different Materials Namely Carbon 70 Steel and Aluminum 7068 by Finite Element Analysis," 2014, [Online]. Available: <https://www.researchgate.net/publication/340429021>
- [6]. P. Mishra and S. Sinha, "Article ID: IJMET_09_09_061 □ Available online at of Connecting Rod of Two Wheelers Using Fea," *International Journal of Mechanical Engineering and Technology (IJMET)*, vol. 9, no. 9, pp. 559–568, 2018, [Online]. Available: <http://iaeme.com/Home/journal/IJMET559editor@iaeme.comhttp://iaeme.com/Home/issue/IJMET?Volume=9&Issue=9http://iaeme.com>.

- [7]. “Analysis and Optimization of Connecting Rod with Different Materials.” [Online]. Available: www.wjrr.org
- [8]. M. Faheem, “ANALYSIS AND OPTIMIZATION OF CONNECTING ROD USING ALFASiC COMPOSITES,” *Int J Innov Res Sci Eng Technol*, vol. 2, 2013, [Online]. Available: www.ijirset.com
- [9]. A. Pandiyan, G. Arunkumar, and G. Premkumar, “Design, analysis and topology optimization of a connecting rod for single cylinder 4–stroke petrol engine,” *International Journal of Vehicle Structures and Systems*, vol. 11, no. 4, pp. 439–442, 2019, doi: 10.4273/ijvss.11.4.20.
- [10]. D. Gopinath and C. V. Sushma, “Design and Optimization of Four Wheeler Connecting Rod Using Finite Element Analysis,” in *Materials Today: Proceedings*, Elsevier Ltd, 2015, pp. 2291–2299. doi: 10.1016/j.matpr.2015.07.267.
- [11]. T. Buddi and R. S. Rana, “Fabrication and finite element analysis of two wheeler connecting rod using reinforced aluminum matrix composites Al7068 and Si3N4,” in *Materials Today: Proceedings*, Elsevier Ltd, 2021, pp. 2471–2477. doi: 10.1016/j.matpr.2020.12.541.
- [12]. A. Patel, “Design Optimization of Connecting Rod for Static Loading Condition,” *International Research Journal of Engineering and Technology*, 2021, [Online]. Available: www.irjet.net
- [13]. M. Faheem, “ANALYSIS AND OPTIMIZATION OF CONNECTING ROD USING ALFASiC COMPOSITES,” *Int J Innov Res Sci Eng Technol*, vol. 2, 2013, [Online]. Available: www.ijirset.com
- [14]. M. K. Lee, H. Lee, T. S. Lee, and H. Jang, “Buckling sensitivity of a connecting rod to the shank sectional area reduction,” *Mater Des*, vol. 31, no. 6, pp. 2796–2803, Jun. 2010, doi: 10.1016/j.matdes.2010.01.010.
- [15]. A. Muhammad, M. A. H. Ali, and I. H. Shanono, “Design optimization of a diesel connecting rod,” 2020. [Online]. Available: www.sciencedirect.com/www.materialstoday.com/proceedings2214-7853
- [16]. P. Dev Srivyas and M. Charoo, “Role Of Fabrication Route On The Mechanical And Tribological Behavior Of Aluminum Metal Matrix Composites-A Review,” 2018. [Online]. Available: www.sciencedirect.com/www.materialstoday.com/proceedings2214-7853
- [17]. J. Chao, “Fretting-fatigue induced failure of a connecting rod,” *Eng Fail Anal*, vol. 96, pp. 186–201, Feb. 2019, doi: 10.1016/j.engfailanal.2018.10.006.
- [18]. O. Parkash, V. Gupta, and V. Mittal \$, “Optimizing the Design of Connecting Rod under Static and Fatigue Loading,” *IJRMST*, 2013. [Online]. Available: www.ijrmst.org
- [19]. T. Sathish, S. Dinesh Kumar, and S. Karthick, “Modelling and analysis of different connecting rod material through finite element route,” in *Materials Today: Proceedings*, Elsevier Ltd, 2020, pp. 971–975. doi: 10.1016/j.matpr.2019.09.139.
- [20]. P. D. Toliya, R. C. Trivedi, and N. J. Chotai, “Design And Finite Element Analysis Of Aluminium-6351 Connecting Rod.” [Online]. Available: www.ijert.org
- [21]. L. Witek and P. Zelek, “Stress and failure analysis of the connecting rod of diesel engine,” *Eng Fail Anal*, vol. 97, pp. 374–382, Mar. 2019, doi: 10.1016/j.engfailanal.2019.01.004.
- [22]. V. B. Kallannavar, V. Chumbre, V. Kallannavar, A. Shirahatti, R. Patil, and S. M. Kerur, “Design and Comparative Analysis of Connecting Rod using Finite Element Analysis Composite View project actual tool life using inverse techniques View project Design and Comparative Analysis of Connecting Rod using Finite Element Analysis,” *SJ Impact Factor*: 6, vol. 887, 2018, [Online]. Available: www.ijraset.com/765
- [23]. N. Panwar and A. Chauhan, “Fabrication methods of particulate reinforced Aluminium metal matrix composite-A review,” in *Materials Today: Proceedings*, Elsevier Ltd, 2018, pp. 5933–5939. doi: 10.1016/j.matpr.2017.12.194.
- [24]. M. Dhanashekar and V. S. Senthil Kumar, “Squeeze casting of aluminium metal matrix composites - An overview,” in *Procedia Engineering*, Elsevier Ltd, 2014, pp. 412–420. doi: 10.1016/j.proeng.2014.12.265.
- [25]. A. R. Pani, R. K. Patel, and G. K. Ghosh, “Buckling analysis and material selection of connecting rod to avoid hydro-lock failure,” in *Materials Today: Proceedings*, Elsevier Ltd, 2019, pp. 2121–2126. doi: 10.1016/j.matpr.2019.09.079.
- [26]. A. Rajugopal Varma and R. Ramachandra, “Design and Analysis of 150CC IC Engine Connecting ROD,” *Accepted*, vol. 8, no. 3, pp. 891–904, 2017, [Online]. Available: www.ijrst.com
- [27]. O. K. Ajayi, B. O. Malomo, S. D. Paul, A. A. Adeleye, and S. A. Babalola, “Failure modeling for titanium alloy used in special purpose connecting rods,” in *Materials Today: Proceedings*, Elsevier Ltd, 2021, pp. 4390–4397. doi: 10.1016/j.matpr.2020.11.852.
- [28]. “Analysis and Optimization of Connecting Rod with Different Materials.” [Online]. Available: www.wjrr.org
- [29]. P. Parida, M. Acharya, A. Purty, and C. Soren, “Analysis of Connecting Rod Under Different Material Condition.” [Online]. Available: www.ijert.org
- [30]. P. Inderchandji Mutha, “To Design a New Cross Section for Connecting Rod with a Target of 10% Weight Reduction,” *International Research Journal of Engineering and Technology*, [Online]. Available: www.irjet.net

➤ Further Reading

- [31]. S. Guleria. 2014. Optimization of steel connecting rod by aluminium connecting rod using finite element analysis, *Int. J. Adv. Res., Ideas and Innovations Tech.*, 1(1), 1-6.
- [32]. “Design of Machine Elements” by V.B. Bhandari, 5th Edition.
- [33]. “Strength of Material” by R.K. Rajput, 10th Edition.